



Influence of free water on dynamic behavior of dam concrete under biaxial compression



Hao Wang^{a,b,*}, Licheng Wang^a, Yupu Song^a, Jizhong Wang^a

^a State Key Laboratory of Coastal and Offshore Engineering, Dalian University of Technology, Dalian, PR China

^b Department of Construction Economics, Liaoning Jianzhu Vocational University, Liaoyang, PR China

HIGHLIGHTS

- Concrete is subjected to biaxial compression under different strain rates.
- The strength of dry and saturated concrete increases with increasing strain rate.
- The strengths and DIF of strengths of dam concretes under dynamic biaxial loading are described.
- The dynamic biaxial compression failure criterion of saturated dam concrete is established.

ARTICLE INFO

Article history:

Received 13 June 2015

Received in revised form 3 January 2016

Accepted 17 February 2016

Available online 2 March 2016

Keywords:

Dam concrete

Experiments

Dynamic strength

Biaxial compression

Saturation

Pore-water

ABSTRACT

The effect of saturation coupled with loading rate on the behavior of dam concrete was investigated under the biaxial compression. Dynamic biaxial compressive experiments on dam concrete cubes with an edge length of 250 mm (dry and saturated) were carried out using a large static and dynamic triaxial electro-hydraulic servo multiaxial testing system. The specimens were loaded in biaxial compressive stress states (with the stress ratios of 0:1, 0.25:1, 0.5:1, 0.75:1 and 1:1 respectively) under static and a series of dynamic loading velocities (with strain rates ranging from 10^{-5} /s to 10^{-2} /s). The ultimate strengths of dry and saturated concretes were found to increase with the increase of strain rate, while the damage pattern and ultimate strength are closely related to the magnitude of lateral pressure exerted on the specimen. In addition, the dynamic failure criterion is proposed to characterize both the effects of strain rate and water content on the ultimate strength of dam concrete under biaxial compressive stress states. By testing dry and saturated specimens, the effect of water content on concrete strength was also examined. The experimental results indicate that the static compressive strengths of saturated concrete are lower than those of concrete in dry state, but on the contrary the dynamic strengths of saturated concrete is higher than those of concrete in dry state. The strain rate effect on strength of saturated concrete is more significant than that of dry concrete in lateral confining pressure, indicating that the saturated concrete is more rate-sensitive than dry concrete. As explained through a basic mechanical analysis, this dissimilarity is mainly attributed to the inertia effect and the viscosity of pore-water inside the saturated concrete during fast (quasi-static or dynamic) loading.

© 2016 Elsevier Ltd. All rights reserved.

1. Introduction

Concrete is one of the most commonly used building materials. It is applied to build house, dam, port, bridge, nuclear safety shell, etc. And concrete structures suffer not only static loads but also dynamic loads such as wave stroke, earthquake, impact, explosion etc. Under such dynamic conditions, the strain-rate causes the

material behavior to be significantly different from what is observed under quasi-static conditions. As well known, strength of concrete depends on the rate of loading, and the values of strength increase as the stress or strain rate increases.

Much research has been conducted since Abrams [1] observed the rate-sensitive behavior of concrete when he carried out compressive tests in 1917. There are many research achievements [2–9] about the rate features of concrete. Bischoff and Perry [10] reviewed the test results of concrete in dynamic compressive loading. Malvar and Ross [11] summarized the test results of concrete in dynamic tensile loading. Bicanic and Zienkiewicz [12] general-

* Corresponding author at: State Key Laboratory of Coastal and Offshore Engineering, Dalian University of Technology, Dalian, PR China.

E-mail address: 830502wh@163.com (H. Wang).

ized the dynamic behavior of concrete based on the experimental results in uniaxial stress state and established dynamic constitutive model.

In recent years, a lot of efforts have been dedicated in the dynamic behavior, only in uniaxial tension and compression. Partly because of the difficulty in conducting multiaxial dynamic experiments, few tests have been reported in the literature concerning the strength and deformation of concrete subjected to varying strain rates and confining pressures. At present, a great deal of experimental research on the deformation and strength of the common small-aggregate concrete has been carried out [13–16], but multiaxial experiments on large-aggregate concrete commonly used in hydraulic engineering are seldom done, except for a few biaxial experiments on large-aggregate concrete carried out by Song et al. [17].

In practical engineering, large-aggregate concrete is often used in hydraulic engineering such as various gravity dams and arch dams, etc. Concrete structures, such as dams, bridge piers, offshore structures, and marine petroleum platforms, often serve in ambient water, and the water content of concrete will have a certain influence on the mechanical behavior. Therefore the concrete could be in saturated or unsaturated states due to water pressure and different types of original defects in the concrete. In the past few decades, many works about the effect of water content on the static properties of concrete have been performed [18–27]. The dynamic mechanical properties of concrete are supposed to be affected by free water in the concrete defects, however very few references about the influence of water content on dynamic properties of concrete could be found. It is very important to conduct special experiments to investigate the mechanical properties of concrete with respect to saturation effect and loading rates in order to facilitate the dynamic performance analysis of hydraulic structures accurately.

As is well known, concrete material is sensitive to the rate of loading. Many studies have been undertaken on the behavior of concrete under uniaxial dynamic loading, as reviewed by Bischoff and Perry [10] for uniaxial compression and by Malvar and Ross [11] for uniaxial tension. However, the dynamic characteristics of concrete under multiaxial stress state are still not well understood due to the lack of experimental data. Only limited dynamic multiaxial experimental studies of concrete under high loading rates have been carried out because of the difficulty for such type of test. From the available literature [28–33], it can be found that the dynamic strength of concrete under multiaxial compressive stress state is also higher than in static state, but the enhancing magnitude is less than that of concrete under uniaxial compressive loading. Consistent conclusions need more experimental and theoretical support. Up to now, researches about the effect of water content on the dynamic behavior of concrete have been focused on the uniaxial state with different moisture content at high strain rates [34,35]. It is shown that the strain rate effect of saturated concrete is more significant than that of normal concrete.

The effect of water content on the behavior of concrete is not taken into account in today's design code. For this reason, it is necessary to carry out experimental investigation into the mechanical behavior of saturated concrete, especially the quasi-static and dynamic characteristics under multiaxial stress state. In this paper, through large numbers of experiments, the strength of dam concrete under the condition of saturation has been studied in the stress state of biaxial compression under different strain rates (10^{-5} – 10^{-2} /s). The experimental results of dry and saturated concrete have been analyzed. By fitting the dam concrete experimental data, the dynamic failure criterion is established in the stress state of biaxial compression.

2. Materials and experimental program

2.1. Materials and mix proportions

The three-graded concrete is commonly used in the upstream face of arch dam. To well match with the real mix proportion of dam concrete in the current study, the size grading of the three-graded coarse aggregate is determined as: large size stone (40–80 mm): mid size stone (20–40 mm): small size stone (5–20 mm) = 4:3:3. This composition of coarse aggregate is a traditional mixture in Chinese code for mix design of hydraulic concrete (DL/T5330-2005), in which the maximum size of the coarse aggregate is set as 80 mm. Meanwhile, the minimum length size of the specimen should not be less than three times of the maximum aggregate size according to the test code for hydraulic concrete (SL352-2006). As a result, the specimens in this paper were all designed as cubes with dimensions $250 \times 250 \times 250$ mm. The cement was ordinary Portland cement, which was produced by Dalian Onoda Cement Plant and one-level fly ash. The mixtures contained fly ash to save cement and to reduce the heat of hydration for practical application. The sand was natural river sand with fineness modulus of 2.6. Table 1 shows the mix proportions by weight of the mixture dam concrete.

2.2. Casting and curing of specimens

The cement, sand, aggregate and fly ash were mixed for about 3 min, then water and water reducer were added, and mixed for two additional minutes. The specimens were vibrated to be dense and solid using a high frequency resistance vibrator. Specimens of 250 mm^3 cube were cast in steel moulds. After 24 h, the specimens were removed from the steel moulds and placed in a condition of $20 \pm 3 \text{ }^\circ\text{C}$ and 95% RH (relative humidity) for 28 days. The six sides of the specimen were ground to ensure that the specimen had flat edges and right-angled corners. The specimens were divided into two batches: one was stored in fresh water till tested, and the other was naturally cured at room condition.

2.3. Apparatus and testing methods

Triaxial testing system used in this project is shown in Fig. 1. The multiaxial experiments were conducted on the servo-hydraulic multiaxial testing system designed by Dalian University of Technology, which made great contributions to the studies of concrete multiaxial constitutive and failure criterion [36–40]. This testing machine is capable of developing three independent compressive or tensile forces. The tensile and compressive loads can reach 1000 kN and 2500 kN, respectively. The loads are applied by means of six loading jacks that were equipped with spherical, self-aligning heads to obtain uniform distribution of stress on the specimens. Forces were measured by the calibrated loading cells with the accuracy of 0.1%. Meanwhile, the deformation was measured by linear variable differential transformer (LVDT) with the accuracy of 0.001 mm.

The regulation circuit for a constant stress-ratio experiment with a constant displacement rate in the major loaded direction was used in the tests. In order to obtain the stable failure modes in the descending stage, the displacement from the output of two LVDTs was employed in computation of strain of the specimens and also used as the feed-back signal to each specimen. The specimens were loaded in biaxial stress states. The lateral pressure was maintained at a fixed proportion to the axial load, with the stress ratios of 0:1, 0.25:1, 0.5:1, 0.75:1, 1:1 respectively. The displacement rates for dam concrete were set as 0.005 mm/s, 0.05 mm/s, 0.5 mm/s and 5 mm/s, which corresponding to the strain rates of 2×10^{-5} /s, 2×10^{-4} /s, 2×10^{-3} /s and 2×10^{-2} /s, respectively. In order to eliminate the restraint induced by the loading platens on the specimen surfaces, the friction-reducing pads [19] were placed between the platens and the specimen for all compressive loading platens. The pads consist of three plastic membranes with two layers of butter between them. For each specific stress ratio, at least three specimens were tested and their average values were used as the presented test results, if it is discrete largely, the numbers of the specimens should be increased and tested.

Table 1
Mix proportion of dam concrete (unit:kg/m³).

Water	Cement	Fly ash	Sand	Aggregate size (mm)			Water reducer
				5–20	20–40	40–80	
120	214	53	549	442.5	442.5	590	0.214



Fig. 1. Photo of the electro-hydraulic servo multiaxial testing system.

3. Test results and discussion

3.1. Average strength

The experimental results of dry and saturated dam concrete at different strain rates under biaxial compression are given in Tables 2 and 3.

3.2. Failure mode

3.2.1. Influence of strain rate

As shown in Fig. 2, different failure modes of specimens with stress ratio equal of 0.5:1 can be observed at different strain rates. The specimen developed a couple of cracks that propagated parallel to the loading direction and were distributed uniformly around the exterior surface under the static loading condition. It is observed that the number of cracks is increased significantly and more microcracks may develop along the major crack as the strain rate increases. For normal strength concrete under loading, the microcracks readily develop and grow along the aggregate–matrix interfaces due to high stress concentrations at these interfaces and due to weak interfacial bonding. These microcracks coalesce and develop into macrocracks under increased loading, leading to a premature failure of concrete compared to mortar. More coarse aggregates are broken along the fracture surfaces with the increase of strain rate. This might be attributed to the fact that when subjected to higher strain rate, cracks do not have enough time to propagate along the path of least resistance; they are forced to propagate through regions of greater resistance, compared to that in lower strain rate. Therefore, more coarse aggregates might be included in the fractured surfaces and a higher stress level is needed to bring the specimens to failure.

Table 2

Average strength of dry dam concrete under dynamic biaxial compression loading (MPa).

Stress ratio	Strain rate (s^{-1})							
	10^{-5}		10^{-4}		10^{-3}		10^{-2}	
	σ_2	σ_3	σ_2	σ_3	σ_2	σ_3	σ_2	σ_3
0:1	0	20.34	0	21.57	0	23	0	24.83
0.25:1	6.63	26.51	6.75	26.98	7.01	28.05	8	32
0.5:1	13.62	27.24	14.63	29.25	15.45	30.9	16.72	33.43
0.75:1	20.06	26.75	20.27	27.03	22.37	29.82	24.65	32.87
1:1	24.69	24.69	26.31	26.31	30.18	30.18	31.15	31.15

Table 3

Average strength of saturated dam concrete under dynamic biaxial compression loading (MPa).

Stress ratio	Strain rate (s^{-1})							
	10^{-5}		10^{-4}		10^{-3}		10^{-2}	
	σ_2	σ_3	σ_2	σ_3	σ_2	σ_3	σ_2	σ_3
0:1	0	17.11	0	26.16	0	24.83	0	27.82
0.25:1	6.19	24.76	6.97	27.89	8.13	32.51	8.74	34.97
0.5:1	13.31	26.62	14.69	29.37	16.41	32.81	15.73	31.45
0.75:1	18.36	24.48	20.99	27.99	23.67	31.56	26.29	35.05
1:1	22.90	22.90	27.79	27.79	29.70	29.70	34.31	34.31

3.2.2. Influence of stress ratio

Fig. 3 demonstrates the failure modes observed for different stress ratios at the strain rate of $10^{-3}/s$. Fracture of the concrete specimens under uniaxial compression is characterized by the formation of a major crack and some minor cracks developing parallel to the direction of applied load. The stress ratio is the major influencing factors of the failure mode. Fracture of the specimens with lateral stress ratios 0.25:1, 0.5:1 and 0.75:1 respectively is characterized by the formation of several major cracks, at an angle of 20–30° to the direction of applied loading. When the specimens are subjected to the biaxial compression with stress ratio equal to 0.75:1, the failure surface of the specimen is flat and parallel to the free surface. It is observed that the failure modes of dam concretes mainly depend on the stress ratio, whereas are independent of the strain rates.

3.3. Stress–strain curves

From Fig. 4, it can be seen that the strength of concrete under biaxial compression increases with the increase of strain rate. The shapes of the stress–strain curves corresponding to different strain rates are similar. The effective modulus for confined specimens is slightly higher than that for unconfined ones. The linear part of the curves extends with the rising strain rate. From stress point higher than 50% strength until peak stress point, the increase in tangent modulus of the curves becomes more pronounced with the rising strain rate in the inelastic range. For concrete specimens, as the strain rate is increased, both the initial slope and the peak stress increase.

3.4. Biaxial compressive strength and dynamic increase factor (DIF)

In Table 2, the ultimate strength of dam concrete in biaxial compression state is higher than the uniaxial compressive strength at any strain rate owing to the effect of lateral confinement. At a specified strain rate, the strength increment depends on the biaxial stress ratio. The maximum biaxial strength occurs at a stress ratio of 0.5 and 0.75 for any strain rate investigated. In a quasi-static test, strength with stress ratio of 0.5:1 is higher than uniaxial compressive strength by about 33.9%. These results are in agreement with the results of other researchers [41–44]. The ultimate strength of concrete under biaxial compression was higher than under uniaxial compression owing to the increased confinement from biaxial compression. It is possible to explain the observed behavior considering that the confinement restrains the crack propagation after the concrete cracks. It also may be attributed to the different grading of aggregate [45], when aggregate particles increase in size, they delay continuous crack growth, extending the period of crack propagation, so the aggregate maximum sizes increase results in a higher increase of ultimate strength.

Relationship between the dynamic strength increment and the strain rate under different stress combinations are shown in Fig. 5. With increasing of the strain rate, the ultimate strength at any

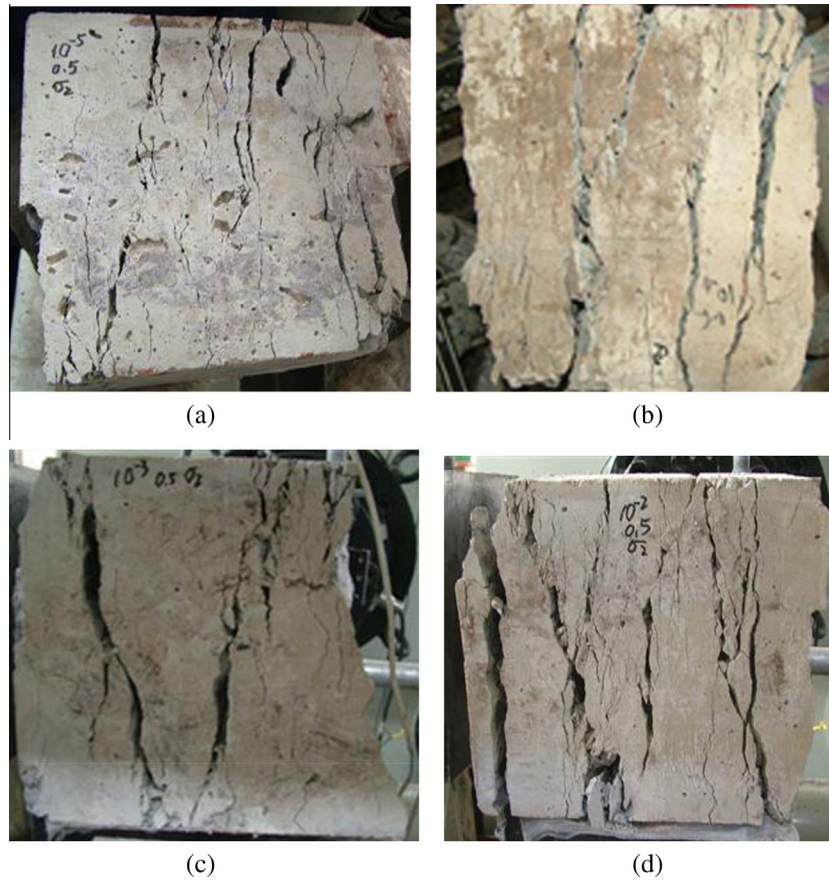


Fig. 2. Typical failure modes of specimens under biaxial compressive stress states ($\alpha = 0.5$) at different strain rates. Strain rates are (a) $10^{-5}/s$; (b) $10^{-4}/s$; (c) $10^{-3}/s$; (d) $10^{-2}/s$ respectively.

stress ratio tends to increase. However, the increment at different stress combinations is not identical. The strain rate was calculated from the linear portion of the strain–time curves in tests. It can be seen from Fig. 5 that the test strength of concrete increased gradually as strain rate increased. In order to formulate the relationship between the strength increment and strain rate, a relationship between the strength and strain rate was established by fitting the test data as follows

$$\frac{f_{bd}}{f_{us}} = a + b \log(\varepsilon/\varepsilon_s) \quad (1)$$

where ε_s is the quasi-static strain rate, its value being selected as $10^{-5}/s$ in this paper; ε is the current strain rate; f_{us} is the uniaxial compressive strength of concrete in quasi-static loading; f_{bd} is the dynamic strength of concrete in biaxial stress state; a , b are parameters depending on the stress ratio. In this study the values of the coefficients a and b , which are determined by the least square method fitting to the test results, are listed in Table 4.

3.5. Effect of water content

3.5.1. Test results for dry and saturated specimens

The test results about dry and saturated specimens under dynamic biaxial compression are shown in Tables 2 and 3 respectively. In this paper, the strain rate of $10^{-5}/s$ is defined as the quasi-static strain rate. The uniaxial compressive strength of saturated concrete at strain rate of $10^{-5}/s$ is less than 15.9% compared to the dry ones. But the uniaxial compressive strength of saturated concrete at strain rate of $10^{-2}/s$ is more than 10.7% compared to the dry ones. The typical stress–strain relationships of saturated

and dry concretes at different strain rates ($10^{-5}/s$, $10^{-3}/s$ and $10^{-2}/s$) under the uniaxial stress state are shown in Fig. 6. The quasi-static strength of saturated concrete decreased compared with those of dry concrete. At strain rate of $10^{-2}/s$, the dynamic critical strain of saturated concrete increased compared with those of dry concrete. The critical strain of both kinds of concretes decreased with the increase of strain rate. The strength of both kinds of concretes increased with the increase of strain rate. The strength of saturated concrete increased more than that of dry concrete. The difference may due to the free water in the concrete.

3.5.2. Comparison of the quasi-static behavior of dried and saturated concretes

Along with the quasi-static results of dry concrete, the quasi-static strength of saturated concrete is given in Fig. 7. It can be seen that the strength of saturated concrete is almost not less than the uniaxial compressive strength, which agree with the condition of dry concrete. Moreover, according to the overall tendency of observation, the ultimate strength of concrete under biaxial compression was higher than under uniaxial compression owing to the increased confinement from biaxial compression. The relative strength increase was dependent on the biaxial stress ratio and the maximum increases occurred at a stress ratio of 0.5 for both dry and saturated concrete. It can be seen the same common characteristics under biaxial compression for both dry and saturated dam concrete. Generally speaking, the strength of saturated concrete is less than the dry ones at any stress ratio.

The quasi-static average strengths of dry and saturated concrete under biaxial compressive are plotted in Fig. 8. Under mechanical confining pressure, the strength of dry concrete shows more signif-

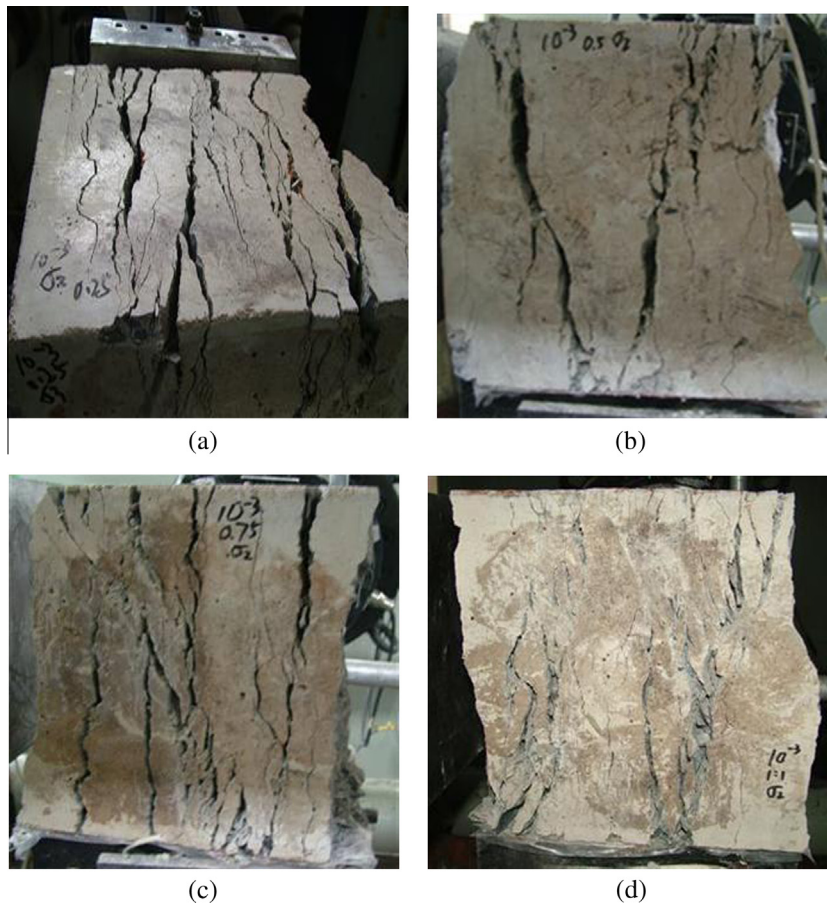


Fig. 3. Typical failure modes of specimens under different stress states at strain rate $10^{-3}/s$ stress ratios are (a) $\alpha = 0.25$; (b) $\alpha = 0.5$; (c) $\alpha = 0.75$; (d) $\alpha = 1$ respectively.

icant confining pressure effect than that of saturated concrete. The normalized strength of dry concrete is higher than that of saturated concrete under the same confining pressure. The strength under confining pressure is much more than the uniaxial compressive strength regardless of dry and saturated concrete. But the quasi-static strength of dry concrete is higher than that of saturated concrete under all the stress ratios. Water pressure within the pore structure of concrete especially developed under the saturated state is responsible for the strength decrease. As mentioned above, the biaxial compression can to different extent increase the strength of the concrete. However, after reaching the ultimate strength, water pressure in the pore structure will also increases. As a result, more cracks may develop and grow on the aggregate–matrix interfaces due to the weak interfacial bonding ability. This procedure will result in the failure (crack accumulation) along the third direction, i.e. perpendicular to the loading surface.

3.5.3. Comparison of the dynamic behavior of dried and saturated concretes

Fig. 9 shows the test results of the dynamic biaxial compressive strength of saturated concrete at different strain rates versus the confining pressure, which indicates that the confining pressure strengthening effects also exist for saturated concrete at different strain rates. The dynamic strength of saturated concrete at biaxial compressive is much more than the dynamic uniaxial compressive strength. The strain rate effect on the strength has a tendency to increase at any stress ratio. From the test results of the Fig. 9, it is noticed that the strength at the same stress ratio in the different strain rates is different. Moreover, the maximum biaxial strength

of the saturated concrete occurs at the stress ratio of 0.5 for any strain rate investigated.

The average strength of dry concrete and saturated concrete under confining pressure are plotted in Fig. 10. The normalized strength of dry concrete is higher than that of saturated concrete under the same confining pressure. Whereas, under dynamic loading, the strength of dry concrete is lower than that of saturated concrete. Increase of the strength for saturated specimens related to the presence of free water.

3.5.4. Influence of free water on the strength of the dam concrete

From test results, it is found that the free water has a major influence on the compressive behavior under high strain rate. The failure of concrete is controlled by the development of cracks. Under the condition of quasi static loading, the volume deformation of concrete lies in compressive state before peak stress. Therefore, free water in the saturated concrete is pushed into the tip of cracks, which acts as a wedge to the crack [46,47]. Under dynamic loading, such as that produced by near-field denotation or ballistic impacts on concrete infrastructure, can generate very high-intensity triaxial stress states in concrete material [48,49]. According to fracture mechanics, the sliding displacement of original crack is proportional to the far field stress, therefore the velocity of sliding or the viscous force of water in the cracks is proportional to the loading rate [50]. Therefore, because of the viscosity of free water and inertia effect, which leads to the enhancement of dynamic strength of saturated concrete based on fracture mechanics.

Under the compressive state, shearing and sliding occurs between original micro inclined cracks. The water in two plates

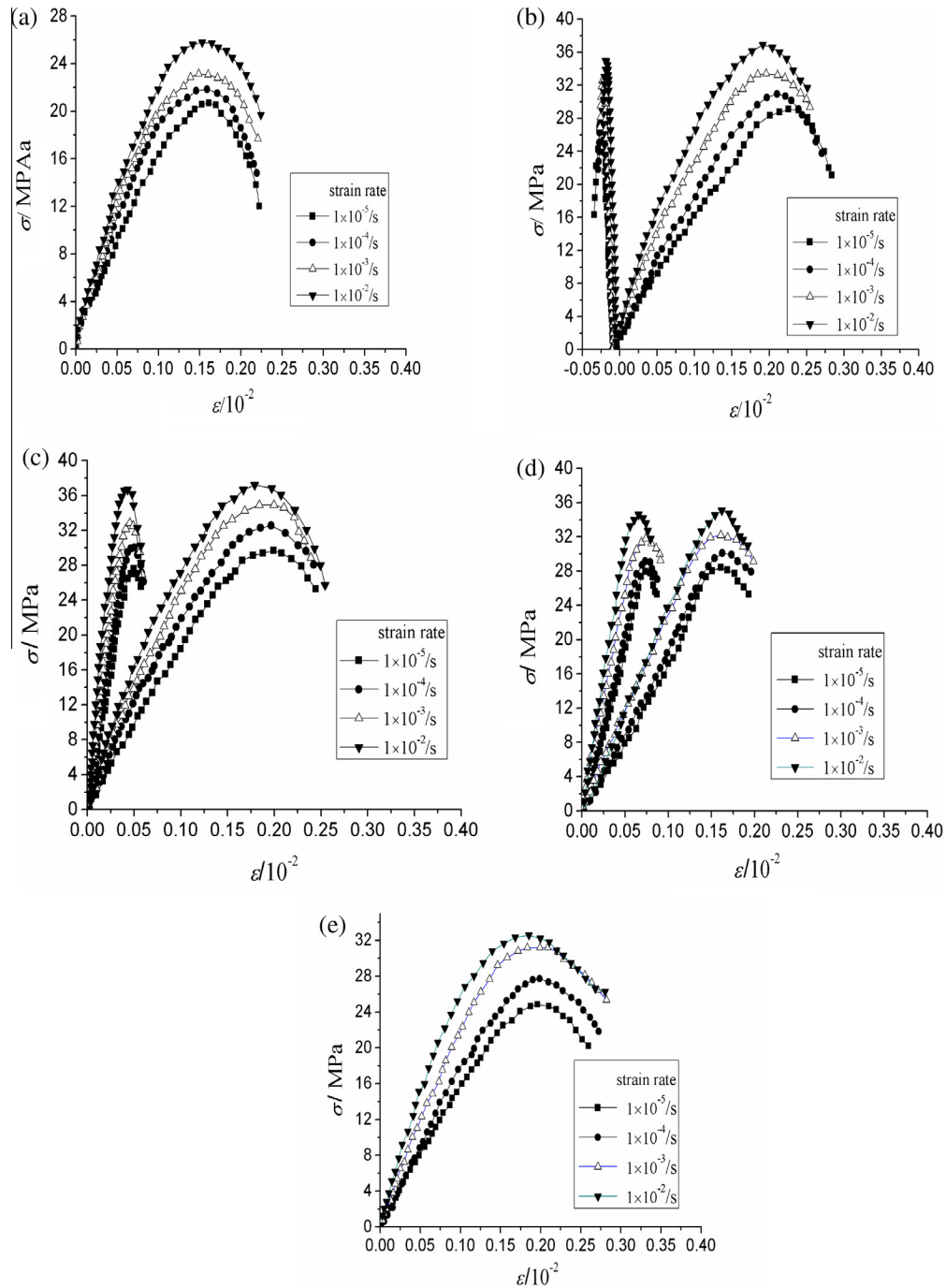


Fig. 4. Stress–strain curves of dry dam concrete at different strain rates. Stress ratios are (a) $\alpha = 0$ (b) $\alpha = 0.25$; (c) $\alpha = 0.5$; (d) $\alpha = 0.75$; (e) $\alpha = 1$ respectively.

acts not as lubricated layer but as resistance force for the relative movement between them. So the water viscosity should affect the properties of concrete. The viscosity of fluid relates not only with the essential property of the fluid, but also with the effective aperture of pores and cracks [51,52]. The influence of water, especially those in micro-scale pores should be taken into account, because the viscosity of water in these pores increases dramatically. Considering this classic case, the phenomenon could be explained by the Newton's equation of viscosity. According to it, the shear stress can be expressed by [53–55]:

$$\tau^w = \frac{F}{A} = \eta \frac{U}{h} = \eta \frac{du}{dy} \quad (2)$$

where F is the loading, A is the area corresponding to F between original micro inclined cracks, U is the velocity due to the loading F , η is the coefficient of water viscosity, $\frac{du}{dy}$ is the velocity gradient, τ^w is the shear stress, the viscous resistance is inversely proportional to the distance h and to the rate of the displacement. According to fracture mechanics, the velocity of sliding or the viscous force of water in the cracks is proportional to the loading rate because of the sliding displacement of original crack is proportional to the far field stress [56].

From Eq. (3), it's clear that the effective shear stress along the original crack is affected by the viscous force which can delays the crack propagation [47].

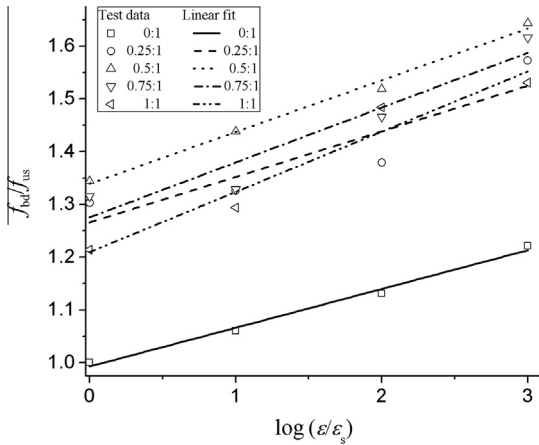


Fig. 5. Relationship between the dynamic strength increment and the strain rate under different stress combinations.

Table 4
Fitting parameters of the linear logarithmic relation.

Stress ratio ($\sigma_2:\sigma_3$)	Fitting parameters		
	a	b	R^2
0:1	0.99	0.0734	0.987
0.25:1	1.27	0.0863	0.737
0.5:1	1.34	0.0981	0.988
0.75:1	1.28	0.104	0.868
1:1	1.21	0.1141	0.924

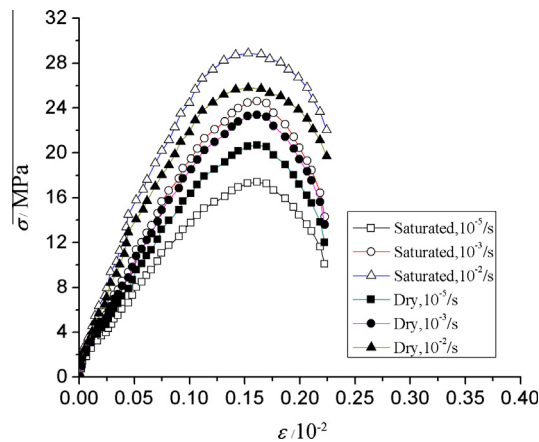


Fig. 6. Stress-strain relationships of saturated and dry dam concrete under the uniaxial stress state.

$$\tau_e = \tau_{dry}^e - f \dot{\sigma} \quad (3)$$

where τ_{dry}^e is the effective shear stress in dry concrete; f is a constant related to the geometry of crack.

Compared with static strength, it can be found that the dynamic compressive strength of concrete increased greatly under high strain rate. A very important factor, which may cause the dynamic strength enhancement of concrete with increase of strain rate, is the free water in the pores of concrete. At low strain rates, the strain rate effect is mainly due to the micro-viscosity mechanism of concrete. Free water in the pores is similar to “wedging effect”, which may accelerate extending of the micro-crack. Thus, free water in the cracks aggravates the damage of concrete. The influence of inertia effect is marginal on the strength of the concrete at low strain rates. Experimental results demonstrate that free

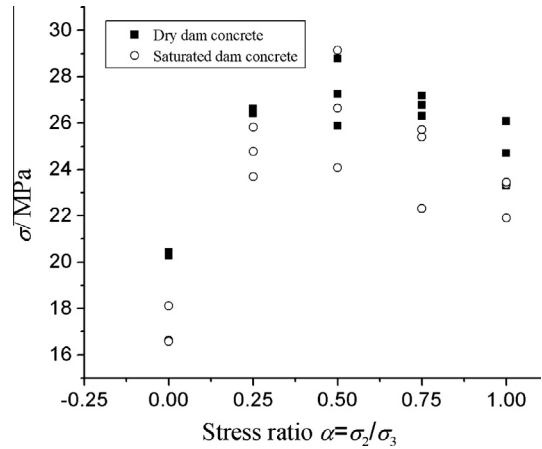


Fig. 7. Static biaxial compressive strength of saturated dam concrete at all stress ratios in comparison with that of dry dam concrete.

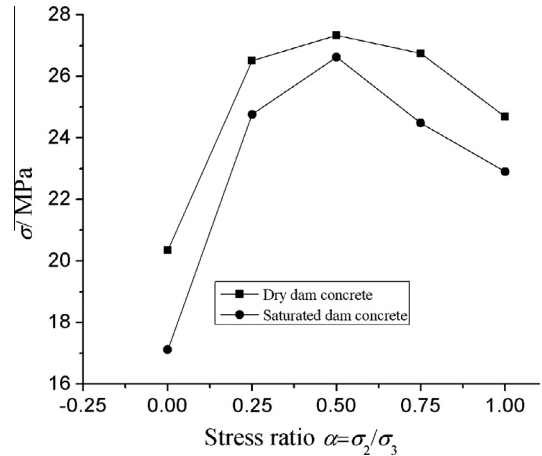


Fig. 8. The quasi-static average strengths of dry and saturated concrete at all the stress ratios.

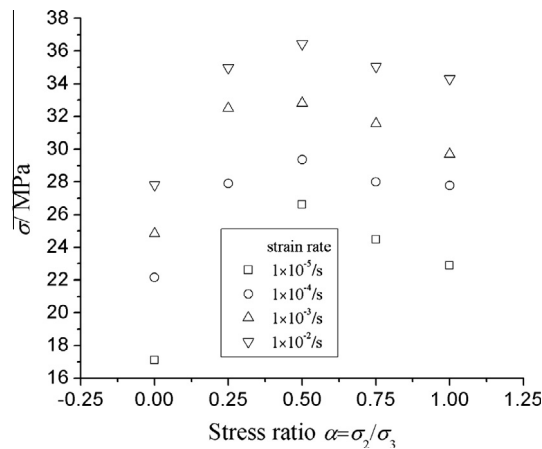


Fig. 9. Dynamic biaxial compressive strength of saturated dam concrete at all the stress ratios.

water in concrete has significant influence on the strain rate effect. The physical background is that under dynamic loading, the flow and transformation of free water in concrete defects induce the damping effect that is similar to the Stefan effect in fluid dynamics. Because of this damping effect, the resistant to micro-crack propa-

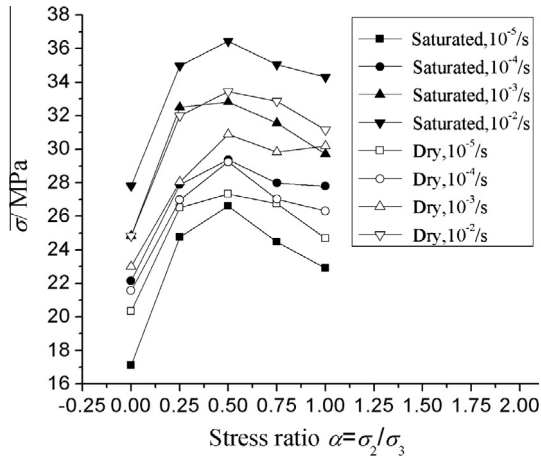


Fig. 10. Dynamic biaxial compressive average strength of saturated dam concrete at all stress ratios in comparison with that of dry dam concrete.

gation is higher under dynamic loading than that under static loads. The lateral confinement comes from both the contact surface restriction and the lateral inertia during rapid compression. However, the stress response of concrete is hydrostatic stress dependent, and therefore, it has completely different response to the lateral confinement. The fact is that the compressive strength of cement-based material can be largely enhanced by the lateral confinement.

For confined compressive tests, saturated materials under compressive loading, the loading does not only result in compression of the solid material, also the pore spaces, and thus the pore water will be compressed. Since the material in confined tests is impermeable, the water can't be drained from the pores and pore pressures in the capillary pores existed. Also though pore air will be compressed, it is claimed that the compressibility of the air is too high to generate noticeable pore air pressures [57]. The term pore pressure is therefore restricted to denote pressures in the pore water. From the Fig. 10, it is found that the strength of fully saturated concrete under lateral confined dynamic compression is larger than the dry ones at strain rates $10^{-4}/s$; $10^{-3}/s$; $10^{-2}/s$, but at strain rates $10^{-5}/s$, it is lower than the dry ones. Under the biaxial compression state of quasi static loading, the free water in the saturated concrete is pushed into the tip of cracks, which acts as a wedge to the crack. While under the dynamic loading, the free water in the concrete along the original crack is affected by the viscous force which can delays the crack propagation.

According to the existing research, the effect of water in concrete has been realized already, but the mechanism is not clear yet [8]. Most of explanations were approached from the physical point of view [56]. It is pointed out that the pore-water in concrete can diminish the internal frictional coefficients [58]. The presence of water in concrete can reduce the effectiveness of Van der Waals attractions, due to the increasing distance between solid gel particles and so secondary bonds diminish [59,60]. From the mechanical point of view, pore-water pressure developed in concrete increases the high stress concentrations at the tip of cracks that will accelerate the damage of concrete. Under high loading rates, the pore pressure is capable of generating tensile strains in concrete and further causing its failure in some cases [61].

Under confining pressure, because of the limitation of two loading directions, cracks developing along the third direction (no loading direction) after reaching ultimate strength, so confining pressure play an important role. Pore-water pressure occurred due to the initial volumetric contraction of the material, reducing the effective lateral stress is defined in the form given below [62]

$$\sigma' = \sigma - pv \tag{4}$$

where σ is the applied lateral confining pressure; p is the pore water pressure built up due to the initial volumetric contraction of the material; and v is the porosity of the material.

In some specific cases, the effective stress is expressed in the following form [63,64]:

$$\sigma_{ij}^e = \sigma_{ij} - \beta p \delta_{ij} \tag{5}$$

where σ_{ij}^e is the plastic effective stress; σ_{ij} is the total stress; β is a plastic effective stress coefficient and less than 1; p is the pore water pressure; and δ_{ij} is the Kronecker symbol.

4. Dynamic strength characteristics in octahedral stress space

The combination of stress invariants is utilized to construct the dynamic strength criterion in which the octahedral stress σ_{oct} , the shear stress τ_{oct} are defined as the normal and shear stress components, respectively, acting on a plane that makes equal angles with each of principal stress directions (called the octahedral stress plane). The direction of the octahedral shear stress τ_{oct} is defined as the angle of similarity θ . The octahedral stresses are calculated by the following equations respectively.

$$\sigma_{oct} = \frac{1}{3}(\sigma_1 + \sigma_2 + \sigma_3) \tag{6}$$

$$\tau_{oct} = \frac{1}{3} [(\sigma_1 - \sigma_2)^2 + (\sigma_1 - \sigma_3)^2 + (\sigma_2 - \sigma_3)^2]^{1/2} \tag{7}$$

$$\theta = \arccos \frac{2\sigma_1 - \sigma_2 - \sigma_3}{3\sqrt{2}\tau_{oct}} \tag{8}$$

For concrete under multiaxial static stress states, the relationship between dynamic normal and shear stresses can has already been proposed as:

$$\frac{\tau_{oct}^d}{f_{us}} = a_1 + a_2 \frac{\sigma_{oct}^d}{f_{us}} + a_3 \log \frac{\dot{\epsilon}}{\dot{\epsilon}_s} \tag{9}$$

where f_{us} is the static uniaxial compressive strength for strain rate of $10^{-5}/s$; σ_{oct}^d and τ_{oct}^d are the dynamic octahedral normal and shear stresses, respectively; a_1 , a_2 and a_3 are the fitting parameters which associated with material properties. By fitting to the test data, a_1 , a_2 and a_3 are determined as 0.402, 0.213 and 0.031 respectively, with the multiple correlation coefficient being 0.928.

The above mentioned relationship in Eq. (9) is depicted in Fig. 11 and the test results are also shown for comparison. It indi-

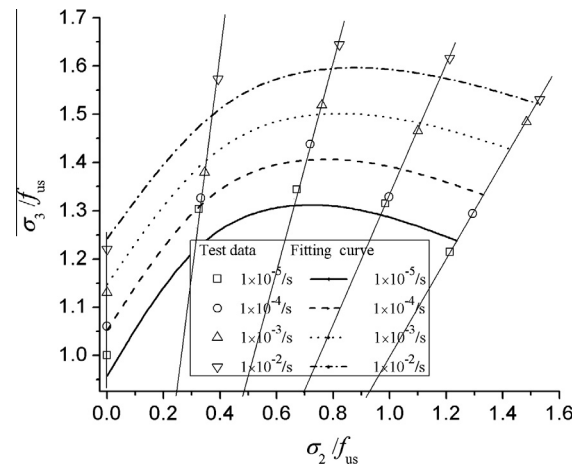


Fig. 11. Strength envelop for dam concrete under biaxial stress.

cates that the Eq. (9) is suitable to express the dynamic biaxial compressive failure criterion. Test results of biaxial compression under the same stress ratio are on the straight lines. It can be seen clearly that the strength of concrete at any given stress ratio (depicting by the straight lines in Fig. 11) increases with the increase of strain rate.

The process of strength reduction in sorption was termed wetting-weakening by Pihlajavaara [18] who proposed a relationship between water content and the uniaxial strength by the form:

$$f_w/f_0 = (1 - cw_r)^{1/2} \quad (10)$$

where f_w is the uniaxial strength of saturated concrete; f_0 is the uniaxial strength of drying concrete; c is a constant; and w_r is the water content.

Because it is difficult to construct a general functional form of failure criteria for the saturated concrete in octahedral stress space, the principal stress space will be considered to develop the failure criteria in order to take into account the influence of water content as well as the effect strain rate. Based on the experimental results of saturated concrete, it can be concluded that the strength enhancement of concrete in biaxial stress states is attributed to both the strain rate and the effect of the water content. A simple expression for the evaluation of dynamic strength of concrete in biaxial stress state is suggested as follows

$$\frac{f_{bd}}{f_{us}} = \left[P_1 + P_2 \log(\dot{\epsilon}/\dot{\epsilon}_s) + \frac{P_3}{(1 + \alpha)^2} + \frac{P_4 \alpha}{(1 + \alpha)^2} \right] (1 - P_5 w_r)^{1/2} \quad (11)$$

where P_1 , P_2 , P_3 , P_4 and P_5 are the fitting parameters which associated with material properties. By fitting to the test data P_1 , P_2 , P_3 , P_4 and P_5 are determined as 1.384, 0.124, -0.184 , -0.184 and -0.482 respectively.

The calculated values of the model for the strength of the concrete in Eq. (11) in Fig. 12 and the test results are also shown for comparison. It can be seen that the calculated strength values for saturated concrete by Eq. (11) are higher than that of the dry concrete. Moreover, one can also note that the predicted results by Eq. (11) match well as a whole with those obtained experimentally. It indicates that the Eq. (11) is suitable to express the dynamic biaxial compressive failure criterion. It should be noted that the proposed strength criterion takes into account the strain-rate effect, the confining pressure effect and the effect of the water content independently and thus it is unable to reflect the coupled effect of strain rate, lateral pressure and the effect of the water content reason-

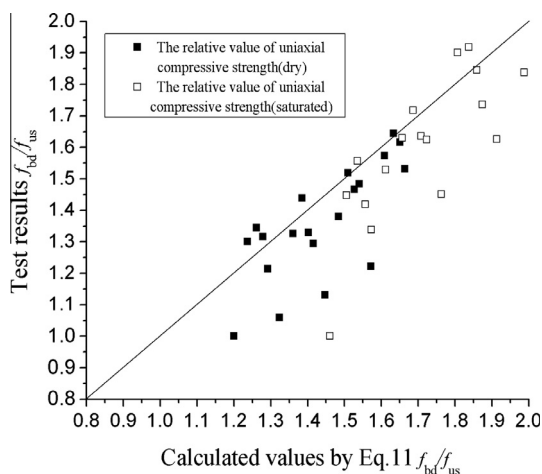


Fig. 12. Comparison between the calculated values by the model of Eq. (11) and the test results.

ably. However, because the test data are somewhat scattered, the proposed strength relation is regarded as acceptable.

These results from the article, in our opinion could draw a final conclusion about the effect of free water on the dynamic compressive strength. However, further studies are still necessary for understanding about the strain-rate effect on multiaxial compressive strength of saturated concrete in dynamic tests.

5. Conclusions

By using the multiaxial dynamic test set-up, a series of biaxial rapid compressive loading tests with five stress ratios α ($\alpha = 0:1, 0.25:1, 0.5:1, 0.75:1, 1:1$) on 120 total specimens were carried out under different strain rates ($10^{-5}/s, 10^{-4}/s, 10^{-3}/s$ and $10^{-2}/s$). Based on the experimental results of dry and saturated concretes under dynamic biaxial stress state, the following conclusions can be drawn:

- (1) The dynamic compressive strength of dry and saturated concrete confined in one lateral direction increases with increasing the strain rate, but the magnitude of increment depends on the lateral stress ratio. The maximum biaxial strength occurs at the stress ratio of $\alpha = 0.5$.
- (2) The strength prediction expression (Eq. (11)) for concrete under biaxial stress state which reasonably reflects both the strain-rate effect and the effect of water content is proposed. The calculated results with this equation are proved to be in good agreement with experimental data.
- (3) The crack patterns and failure modes of the specimens observed in the dynamic experiments with strain rates ranging from $10^{-5}/s$ to $10^{-2}/s$ are very similar to those observed in static experiments. It is also found that the failure modes and crack patterns of the specimens are predominantly controlled by the lateral stress ratio and almost not affected by the strain rate.
- (4) The static compressive strengths of saturated concrete are lower than those of the dry concrete at all the stress ratios involved in the current study. On the contrary, however, the dynamic compressive strengths of saturated concrete are higher than those of the dry concrete under high strain rate. This implies that the strain rate effect on the strength of saturated concrete is more significant than that of the dry concrete, especially when subjected to the lateral confinement. Thus it can be concluded that the saturated concrete is more rate-sensitive than dry concrete. The inertia effect and the viscosity of pore-water within concrete are regarded as the two main factors to induce the enhancement of dynamic strength of saturated concrete.

Acknowledgments

This research is supported by the National Natural Science Foundation of China (Grant No. 51079019; 51378090) and the National Key Basic Research Program of China (973 Program) (No. 2015CB057703; 2015CB057701). The authors gratefully acknowledge the financial supports.

References

- [1] A.D. Abrams, Effect of rate of application of load on the compressive strength of concrete, *J. ASTM* 17 (1917) 364–377.
- [2] W. Goldsmith, M. Polivka, T. Yang, Dynamic behavior of concrete, *Exp. Mech.* 6 (1966) 65–79.
- [3] P. Rossi, Dynamic behaviour of concretes: from the material to the structure, *Mater. Struct.* 27 (1994) 319–323.
- [4] S.Y. Xiao, G. Lin, J.Z. Lu, Z. Wang, Effect of strain rate on dynamic behavior of concrete in compression, *J. Harbin Univ. Civil Eng. Arch.* (2002) 35–39.

- [5] A. Brara, J.R. Klepaczko, Experimental characterization of concrete in dynamic tension, *Mech. Mater.* 38 (2006) 253–267.
- [6] I.E. Shkolnik, Influence of high strain rates on stress–strain relationship, strength and elastic modulus of concrete, *Cem. Concr. Compos.* 30 (2008) 1000–1012.
- [7] D. Yan, G. Lin, Influence of initial static stress on the dynamic properties of concrete, *Cem. Concr. Compos.* 30 (2008) 327–333.
- [8] Z. Chen, Y. Hu, Q. Li, M. Sun, P. Lu, T. Liu, Behavior of concrete in water subjected to dynamic triaxial compression, *J. Eng. Mech.* 136 (2010) 379–389.
- [9] Shajie, Zeng, Xiaodan, Ren, Jie, Li, Triaxial behavior of concrete subjected to dynamic compression, *J. Struct. Eng.* 139 (2013) 1582–1592.
- [10] P.H. Bischoff, S.H. Perry, Compressive behaviour of concrete at high strain rates, *Mater. Struct.* 24 (1991) 425–450.
- [11] J. Malvar, A. Ross, Review of strain rate effects for concrete in tension, *ACI Mater. J.* 95 (1998) 435–439.
- [12] N. Bicanic, O.C. Zienkiewicz, Constitutive model for concrete under dynamic loading, *Earthquake Eng. Struct. Dyn.* 5 (1983) 689–710.
- [13] Z.H. Guo, *Strength and Deformation of Concrete: Test Foundation and Constitutive Relationship*, Tsinghua University Press, Beijing, China, 1997 [in Chinese].
- [14] Y.P. Song, *Failure Criteria and Constitutive Relations of Concrete*, Water Power Press, Beijing, China, 2002 [in Chinese].
- [15] H. Kupfer, H.K. Hilsdorf, H. Rusch, Behavior of concrete under biaxial stresses, *ACI J. Proc.* 66 (1969) 656–666.
- [16] L.H. Jiang, D.H. Huang, N.X. Xie, Behavior of concrete under compressive–tensile stresses, *ACI Mater. J.* 88 (1991) 181–185.
- [17] Y.P. Song, G.F. Zhao, Failure criterion of the mass concrete under combined compression–tension stress states. in: *Proceedings of 6th International Offshore and Polar Engineering conference*, ISOPE, Golden, CO, USA, 1996, 5, pp. 26–31.
- [18] S.E. Pihlajavaara, A review of some of the main results of a research on the aging phenomena of concrete: effect of moisture conditions on strength, shrinkage and creep of mature concrete, *Cem. Concr. Res.* 4 (1974) 761–771.
- [19] S. Popovics, Effect of curing method and final moisture condition on compressive strength of concrete, *J. Am. Concr. Inst.* 83 (1986) 650–657.
- [20] F.M. Barlett, J.G. MacGregor, Effect of moisture condition on concrete core strength, *ACI Mater. J.* 91 (1993) 227–236.
- [21] J. Glucklich, U. Korin, Effect of moisture content on strength and strain energy release rate of cement mortar, *J. Am. Ceram. Soc.* 58 (1975) 517–521.
- [22] N. Burlion, F. Bourgeois, J.F. Shao, Effect of desiccation on mechanical behavior of concrete, *Cem. Concr. Compos.* 27 (2005) 367–379.
- [23] V. Kanna, R.A. Olson, H.M. Jennings, Effect of shrinkage and moisture content on the physical characteristics of blended cement mortars, *Cem. Concr. Res.* 28 (1998) 1467–1477.
- [24] D.J. Cook, M.N. Haque, The effect of sorption on the tensile creep and strength reduction of desiccated concrete, *Cem. Concr. Res.* 4 (1974) 367–379.
- [25] I. Yurtdas, N. Burlion, F. Skoczylas, Experimental characterization of the drying effect on uniaxial mechanical of mortar, *Mater. Struct.* 37 (2004) 170–176.
- [26] I. Yurtdas, N. Burlion, J.F. Shao, A. Li, Evolution of the mechanical behavior of a high performance self-compacting concrete under drying, *Cem. Concr. Compos.* 33 (2011) 380–388.
- [27] X.H. Vu, Y. Malecot, L. Daudeville, E. Buzaud, Experimental analysis of concrete behavior under high confinement: effect of the saturation ratio, *Int. J. Solids Struct.* 46 (2009) 1105–1120.
- [28] J. Takeda, H. Tachikawa, K. Fujimoto, Mechanical behavior of concrete under higher rate loading than in static test, *Mech. Mater., Soc. Mater. Sci.* 2 (1974) 479–486.
- [29] H. Yamaguchi, K. Fujimoto, S. Nomura, Strain rate effect on stress–strain relationships of concrete. in: *Proc., 4th Symp. on the Interaction of Non-nuclear Munitions with Structures*, Panama City Beach, FLA, 1989, pp. 290–295.
- [30] J.K. Gran, A.L. Florence, J.D. Colton, Dynamic triaxial tests of high-strength concrete, *J. Eng. Mech. Div.* 115 (1989) 891–904.
- [31] Q.H. Ju, M.B. Wu, Experimental studies of dynamic characteristic of rocks under triaxial compression, *J. Geotech. Eng.* 15 (1993) 73–80 [in Chinese].
- [32] K. Fujikake, K. Mori, K. Uebayashi, et al., *Dynamic Properties of Concrete Materials with High Rates of Tri-axial Compressive Loads*, WIT Press, Southampton, U.K., 2000.
- [33] D.M. Yan, Experimental and theoretical study on the dynamic properties of concrete Ph.D. thesis, Dalian Univ. of Technology, Dalian, China, 2006.
- [34] P. Rossi et al., The dynamic behavior of concrete: Influence of free water, *Mater. Struct.* 25 (1992) 509–514.
- [35] C.A. Ross, D.M. Jerome, J.W. Tedesco, et al., Moisture and strain rate effects on concrete strength, *ACI Mater. J.* 93 (1996) 293–300.
- [36] H.L. Wang, Y.P. Song, Behavior of dam concrete under biaxial compression–tension and triaxial compression–compression–tension, *Mater. Struct.* 42 (2009) 241–249.
- [37] H.S. Shang, Y.P. Song, Experimental study of strength and deformation of plain concrete under biaxial compression after freezing and thawing cycles, *Cem. Concr. Res.* 36 (2006) 1857–1864.
- [38] H.S. Shang, Y.P. Song, Performance of plain concrete under biaxial tension–compression after freeze–thaw cycles, *Mag. Concr. Res.* 62 (2010) 149–155.
- [39] Z.J. He, Y.P. Song, Triaxial strength and failure criterion of plain high-strength and high-performance concrete before and after high temperatures, *Cem. Concr. Res.* 40 (2010) 17–18.
- [40] H.S. Shang, Triaxial T–C behavior of air-entrained concrete after freeze–thaw cycles, *Cold Reg. Sci. Technol.* 89 (2013) 1–6.
- [41] H. Kupfer, K.H. Gerstle, Behavior of concrete under biaxial stresses, *J. Eng. Mech. Div., ASCE* 99 (1973) 852–866.
- [42] S.K. Lee, Y.C. Song, S.H. Han, Biaxial behavior of plain concrete of nuclear containment building, *Nucl. Eng. Des.* 2 (2004) 143–153.
- [43] J.K. Gran, A.L. Florence, J.D. Colton, Dynamic triaxial tests of high-strength concrete, *Eng. Mech.* 115 (1989) 891–904.
- [44] D. Yan, G. Lin, Dynamic behaviour of concrete in biaxial compression, *Mag. Concr. Res.* 59 (2007) 45–52.
- [45] H.L. Wang, Y.P. Song, Biaxial compression behavior of different aggregate graded concrete, *Mag. Concr. Res.* 61 (2009) 457–463.
- [46] H.L. Wang, Q.B. Li, Mesomechanics analysis of compressive strength and constitutive equation of wet concrete, *J. Rock Mech. Eng.* 25 (2006) 1531–1536 [in Chinese].
- [47] H.L. Wang, W.L. Jin, Q.B. Li, Saturation effect on dynamic tensile and compressive strength of concrete, *Adv. Struct. Eng.* 12 (2009) 279–286.
- [48] X.H. Vu, Y. Malecot, L. Daudeville, Strain measurements on porous concrete samples for triaxial compression and extension tests under very high confinement, *J. Strain Anal. Eng.* 44 (2009) 633–657.
- [49] X.H. Vu, Y. Malecot, L. Daudeville, E. Buzaud, Effect of the water/cement ratio on concrete behavior under extreme loading, *Int. J. Numer. Anal. Met.* 33 (2009) 1867–1888.
- [50] H.L. Wang, Q.B. Li, Prediction of elastic modulus and Poisson's ratio for unsaturated concrete, *Int. J. Solids Struct.* 44 (2007) 1370–1379.
- [51] P.K. Mehta, P.J.M. Monteiro, *Concrete: Microstructure Properties and Materials*, Indian Concrete Institute, 1997.
- [52] K. Maekawa, R. Chaube, T. Kishi, *Modeling of Concrete Performance. Hydration, Microstructure Formation and Mass Transport*, E & FN Spon, 1999.
- [53] E.J. Finnemore, J.B. Franzini, *Fluid Mechanics with Engineering Applications*, McGraw-Hill Companies Inc Press, USA, 2002.
- [54] J.H. Spurk, *Fluid Mechanics*, Springer-Verlag Press, Berlin Heidelberg, Germany, 1997.
- [55] V.L. Streeter, E.B. Wylie, K.W. Bedford, *Fluid Mechanics*, McGraw-Hill Companies Inc Press, USA, 1998.
- [56] L.J. Lima, D. Violini, R. Zerbinio, *Fracture Toughness and Fracture Energy of Concrete*, Elsevier Science, Amsterdam, 1986, pp. 219–222.
- [57] F. Skoczylas, N. Burlion, I. Yurtdas, About drying effects and poro-mechanical behaviour of mortars, *Cem. Concr. Compos.* 29 (2007) 383–390.
- [58] A.M. Neville, *Properties of Concrete*, Wiley Press, New York, USA, 1996.
- [59] P.L. Domone, Uniaxial tensile creep and failure of concrete, *Mag. Concr. Res.* 26 (1974) 144–152.
- [60] R.H. Mills, Effects of sorbed water on dimensions, compressive strength, and swelling pressure of hardened cement pastes, *Highway Res. Board* 90 (1966) 84–111.
- [61] J.E. Butler, The influence of pore pressure upon concrete, *Mag. Concr. Res.* 33 (1981) 3–17.
- [62] I. Imran, S.J. Pantazopoulou, Experimental study of plain concrete under triaxial stress, *ACI Mater. J.* 93 (1996) 589–601.
- [63] P. De Buhan, L. Dormieux, On the validity of the effective stress concept for assessing the strength of saturated porous materials: a homogenization approach, *J. Mech. Phys. Solids* 44 (1996) 1649–1667.
- [64] D. Lydzba, J.F. Shao, Stress equivalence principle for saturated porous media, *Mag. Concr. Res.* 330 (2002) 297–303.